An improved approach to the problem of nonlinear electrostatic structures in plasma columns

H. Ramachandran

Citation: Physics of Plasmas (1994-present) **8**, 1910 (2001); doi: 10.1063/1.1350573
View online: http://dx.doi.org/10.1063/1.1350573
View Table of Contents: http://scitation.aip.org/content/aip/journal/pop/8/5?ver=pdfcov
Published by the AIP Publishing

An improved approach to the problem of nonlinear electrostatic structures in plasma columns*

H. Ramachandran[†,a)]
Institute for Plasma Research, Bhat, Gandhinagar 382 428, India

(Received 25 October 2000; accepted 14 December 2000)

An improved method of solving for the structure of nonlinear electrostatic structures in plasma columns is presented. The fully nonlinear solution of the Trivelpiece–Gould (GT) mode has been obtained both for the case where the perpendicular mode structure is held constant and for the case where it is a function of the nonlinear amplitude. Unlike conventional approaches, the perpendicular structure of the mode is permitted to vary with amplitude. Temperature effects and radial profile effects are included in this treatment. The results are compared with those obtained if the perpendicular eigenmode is held constant and with the literature. © *2001 American Institute of Physics.* [DOI: 10.1063/1.1350573]

I. INTRODUCTION

Nonlinear structures are commonly observed in plasma systems and plasma columns are no exception. At the low frequency end, ion-acoustic structures are observed in neutral plasma columns. At higher frequencies, electron solitary waves are observed[1–3] that are the nonlinear development of the Trivelpiece–Gould (GT) mode.[4] The common understanding of these modes is that the perpendicular response of the modes is linear while the nonlinear effects are seen in the parallel response. The resulting equation has been solved with different kinds of approximations to yield solitary waves.[1,2,5] These approaches have attempted to deal with the nonlinear parallel response while retaining the perpendicular response as linear. The problem has also been explored by the direct solution of the two-dimensional (2D) Poisson equation[6] and through a $2\frac{1}{2}$D particle-in-cell (PIC) simulation.[7] These numerical studies found that the perpendicular profile remains close to the undistorted value, and concluded that the existing techniques were acceptable. However, the numbers from these two studies did not agree with each other and with experiments.

In this paper, an alternate approach to the analysis of GT waves is presented that improves on the existing treatments, not only of the parallel nonlinearity but also includes the effects of nonlinearity in the perpendicular response. The next section presents an exact treatment of the parallel nonlinearity for the case where the perpendicular mode structure can be treated as undistorted. Closed form solutions are obtained that compare well with the numerical calculations. Section III extends the results to the case of warm plasma columns. Section IV then introduces a method to include nonlinear effects in the perpendicular response as well. The method is applied to various interesting configurations to generate solutions that take temperature as well as radial profiles into account. The results are found to be in agreement with most of the existing results in the relevant limits, and provides a means to interpret the various studies. The paper concludes with Sec. V, where the technique developed here is reviewed for its general applicability to similar problems.

II. AN EXACT TREATMENT OF THE PARALLEL NONLINEARITY FOR THE CASE OF LINEARIZED PERPENDICULAR RESPONSE

The problem of the nonlinear GT mode propagating in a strongly magnetized plasma column that is axially infinite (see Fig. 1 for schematic) is best discussed via the theory of Bernstein–Greene–Kruskal (BGK)[8] modes. In the frame of the solitary wave, the potential structure is time invariant, and the energy of a particle, E, becomes a conserved quantity. The electron and ion distributions can therefore be described as functions of E alone. For GT modes, we simplify further by treating the ions as stationary, i.e., $n_i \equiv n_0$ where n_0 is the plasma density in the absence of the wave. For a cold plasma column, therefore, the plasma charge density at any point is given by $\rho = e n_0 (1 - 1/\sqrt{1+\tilde{\phi}/M^2})$, where $\tilde{\phi} = 2e(\phi - \phi_0)/m_e u_{\mathrm{GT}}^2$ is the change in potential due to the wave normalized to $m u_{\mathrm{GT}}^2/2$ and $M^2 = u_0^2/u_{\mathrm{GT}}^2$ is the Mach number of the solitary wave. Here, $-e$ and m_e are the charge and mass, respectively, of electrons, and u_{GT} is the Trivelpiece–Gould velocity[4] of the wave. In the frame of the wave, u_0 appears as the asymptotic velocity of the incoming electron beam. If the column were non-neutral, the ion contribution would be missing. Poisson's equation becomes

$$\nabla_\perp^2 \psi + \frac{\partial^2 \psi}{\partial \zeta^2} = P\left[1 - \frac{1}{\sqrt{1-\psi}}\right], \tag{1}$$

where $\psi = \tilde{\phi}/M^2$ is the fraction of the potential to its wave-breaking value, and the coordinates $(\rho, \zeta) = (r/a, z/a)$ have been normalized to the inner radius of the boundary. $P = 2\omega_{pe}^2 a^2/u_0^2$ is the main parameter of this nonlinear problem. Other parameters appear through the perpendicular profile of the plasma, but for a uniform plasma cylinder in an infinite magnetic field, P completely characterizes the non-

*Paper UI2 2, Bull. Am. Phys. Soc. **45**, 291 (2000).
†Invited speaker.
a)Electronic mail: hari@ipr.res.in

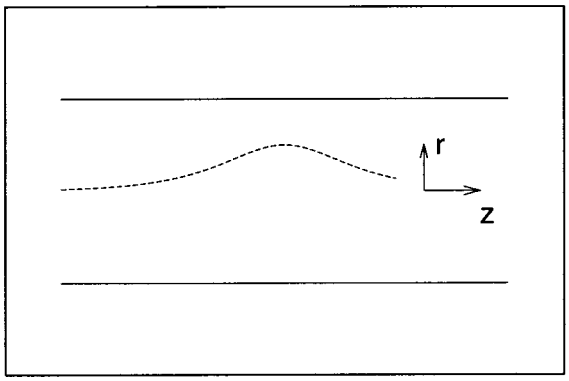

FIG. 1. Geometry of the system under study. An infinite axial magnetic field is assumed present and the boundary at $r=a$ is grounded. The background plasma properties are assumed to depend only on r.

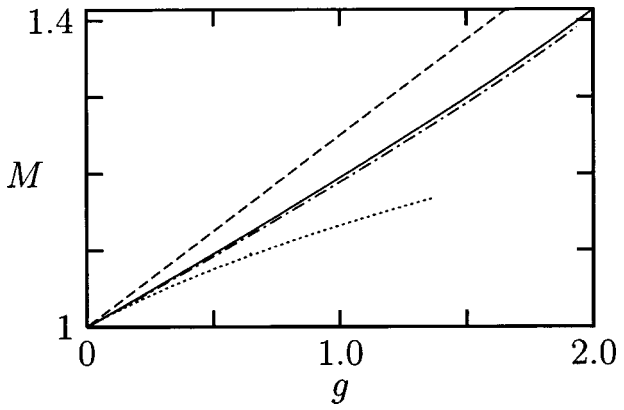

FIG. 2. Figure showing the normalized velocity of the solitary wave as a function of its normalized peak potential. The solid line is Eq. (9). The dotted–dashed line comes from the solution of Eq. (7). The dotted line is the result of truncating the nonlinearity to order that yields the KdV equation. The dashed line is from Ref. 5, Eq. (7).

linear problem. It should be noted that Eq. (1) is applicable to both neutral and non-neutral plasma columns. In the neutral case, the factor of 1 inside the square brackets represents the ion charge and in the non-neutral case, it represents the equilibrium charge density of the plasma column.

The linear theory of the GT mode can be obtained from Eq. (1) by expanding the right-hand side of the equation

$$\frac{1}{\rho}\frac{\partial}{\partial\rho}\left(\rho\frac{\partial\psi}{\partial\rho}\right)-k_{\|}^2\psi=-\frac{P}{2}\psi. \tag{2}$$

This equation is for the θ-symmetric mode, and its solution is $\psi=g(\zeta)J_0(\lambda_{01}\rho)$. The term on the right-hand side of Eq. (2) is what permits an oscillatory solution along ζ. When the mode is nonlinear, the right-hand side of Eq. (1) yields sufficient charge density to make the solution oscillatory near the peak of the structure, but is underdense in the tail. Thus, the far away regions are exponential along ζ.

Using the separability ansatz, $\psi(\rho,\zeta)=g(\zeta)\psi_\perp(\rho)$, Eq. (1) can be reduced to an equation in ζ by applying $\langle\psi_\perp|$ to the equation:

$$\frac{d^2g}{d\zeta^2}-k_\perp^2 g=-\frac{\left\langle\psi_\perp\middle|P\left[\dfrac{1}{\sqrt{1-g\psi_\perp}}-1\right]\right\rangle}{\langle\psi_\perp|\psi_\perp\rangle}. \tag{3}$$

Here, P has been left inside the averaging operator since it may, in general, be a function of ρ. Equation (3) can be reduced to potential form

$$\frac{1}{2}\left(\frac{dg}{dz}\right)^2-\frac{k_\perp^2g^2}{2}=-\frac{\left\langle\psi_\perp\middle|P\left[\dfrac{2}{\psi_\perp}(1-\sqrt{1-g\psi_\perp})-g\right]\right\rangle}{\langle\psi_\perp|\psi_\perp\rangle}. \tag{4}$$

The effective potential, $V_g(g)$, corresponding to Eq. (4) is given by

$$V_g(g)=-\frac{k_\perp^2g^2}{2}+\frac{\left\langle\psi_\perp\middle|P\left[\dfrac{2}{\psi_\perp}(1-\sqrt{1-g\psi_\perp})-g\right]\right\rangle}{\langle\psi_\perp|\psi_\perp\rangle}. \tag{5}$$

The zeros of $V_g(g)$ yield the solitary wave amplitude. To connect the amplitude of the wave to its speed, we take the linear limit of Eq. (5):

$$V_g(g)=\left(-\frac{k_\perp^2}{2}+\frac{P_0\alpha}{4}\right)g^2+\mathcal{O}(g^3), \tag{6}$$

where $\alpha=\langle\psi_\perp|P\psi_\perp\rangle/P_0\langle\psi_\perp|\psi_\perp\rangle$ and P_0 is the on-axis value of P. $k_\perp$ and $P_0\alpha$ are connected by the requirement $k_\perp^2\geqslant P_0\alpha/2$. The amplitude must go to zero in the linear limit, which requires that the coefficient of g^2 becomes zero. Simultaneously, the velocity u_0 becomes the GT velocity. Thus, $2k_\perp/P_0\alpha=P_{0\,\max}/P_0=u_0^2/u_{\mathrm{GT}}^2=M^2$. Equation (5) therefore becomes

$$\frac{V_g(g)}{P_0\alpha}=-\frac{M^2g^2}{4}+\frac{\left\langle\psi_\perp\middle|P\left[\dfrac{2}{\psi_\perp}(1-\sqrt{1-g\psi_\perp})-g\right]\right\rangle}{\langle\psi_\perp|P\psi_\perp\rangle}. \tag{7}$$

Since $V_g(g)$ is zero at the peak of the wave, Eq. (7) immediately yields the connection between M, the Mach number of the wave, and g_0, its normalized peak potential, for the fully nonlinear GT mode.

Figure 2 presents the M vs $\tilde{\phi}_0=g_0M^2$ curve for the case of a uniform background (i.e., $\alpha=1$). The dotted–dashed line is obtained by numerically evaluating Eq. (7) using $\psi_\perp=J_0(\lambda_{01}\rho)$. Also plotted is the result obtained if the nonlinearity is only kept to $\mathcal{O}(g^3)$. The dashed line is the result of [Ref. 5, Eq. (7)]. If $\psi_\perp$ is approximated by $1-\rho^2$, the integrals in Eq. (7) can be done explicitly, yielding

$$\frac{V(g)}{P_0\alpha}=-\frac{M^2g^2}{4}+\left[\frac{4(1-g)^{3/2}}{g}-\frac{4}{g}+6-\frac{3g}{2}\right]. \tag{8}$$

The $M(\tilde{\phi})$ curve is obtained from setting $V(g_0)$ in Eq. (8) to zero

$$M^2=\frac{16(1-g)^{3/2}-16+24g-6g^2}{g^3}. \tag{9}$$

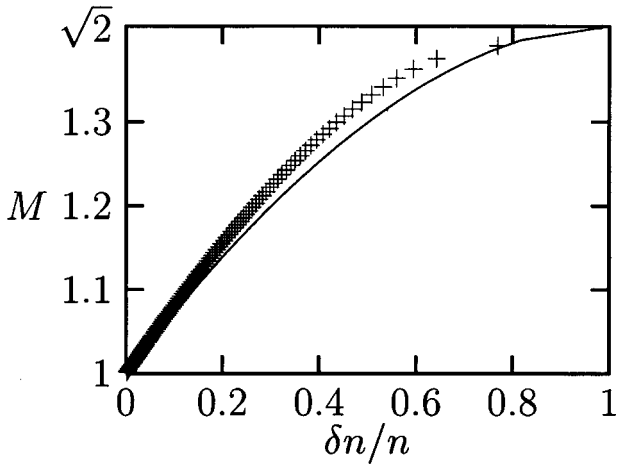

FIG. 3. The same data in Fig. 2 plotted against charge content (normalized to background charge in electrons). The + symbols represent the result obtained by numerically integrating Eq. (10) while the solid line is the result of using Eq. (11).

This is the solid line plotted in Fig. 2. The result is extremely close to the value obtained by numerically evaluating Eq. (7) with $J_0(\lambda_{01}\rho)$ as the eigenmode.

Since the experimental diagnostic in non-neutral systems to detect such waves is the capacitive probe, it is of interest to know the fractional change in charge that corresponds to a value of g. The charge content per unit length in the column for a radial profile that is uniform is given by $\int_0^1 \rho\, d\rho = -1/2$ in normalized units. The additional charge added by the presence of the wave is given by

$$\int_0^1 \rho\left(1-\frac{1}{\sqrt{1-g\,\psi_\perp}}\right)d\rho. \tag{10}$$

The integral can be evaluated for $\psi_\perp = 1-\rho^2$ to yield

$$\frac{\delta n}{n_0} = \frac{1}{g}[2(1-\sqrt{1-g})-g]. \tag{11}$$

The plot of $M(\delta n/n)$ is presented in Fig. 3. The + symbols correspond to $\psi_\perp = J_0(\lambda_{01}\rho)$ while the solid line is the result of Eq. (11). The non-neutral result (Ref. 3, Fig. 6 and text following) is that $M=1.07$ for $\delta n/n = 0.1$. This is in agreement with both curves in Fig. 3. However, this agreement should be treated with caution, since the experiment had the plasma filling only a quarter of the volume of the chamber. The effect of a radial profile will be examined later in this paper, but to anticipate the findings, it appears that the nonlinearly correct solution for a case where the plasma fills a quarter of the volume roughly agrees with the simple analysis of this section for the uniform case (i.e., $\alpha=1$).

III. INCLUDING TEMPERATURE EFFECTS

The cold beam treatment of GT waves is quite successful in explaining most of the experimental features observed, where the nonlinearity is weak. However, the fully nonlinear wave structure is dominated by the singularity in the charge density in Eq. (1). This singularity is removed if temperature effects are present. This section presents an analytic formula for the charge density that includes the effects of temperature. The formula is derived not for a Maxwellian, however, but for a Lorentzian distribution. Numerically, there is no difficulty in treating a Maxwellian distribution. The use of the Lorentzian model has been for the sake of extracting an explicit expression for the charge density.

The electron distribution in the wave frame is assumed to be

$$f(E) \propto \frac{1}{(E-E_0)^2+\delta^2}, \tag{12}$$

where δ is the energy spread in the beam. The fractional charge density, $\Lambda(\psi)$, is then determined by the integral

$$\Lambda(\psi) = C_0 \int_\psi^\infty \frac{1}{[(1-E)^2+\Delta^2]\sqrt{E-\psi}}\,dE, \tag{13}$$

where C_0 is a normalization constant and all quantities have been normalized with respect to E_0, the central energy of the beam. This integral can be obtained in closed form and yields

$$\Lambda(\psi) = \sqrt{\frac{1+\Delta^2}{(1-\psi)^2+\Delta^2}\,\frac{\sqrt{1+\Delta^2}-1}{\sqrt{(1-\psi)^2+\Delta^2}-(1-\psi)}}-1. \tag{14}$$

It is simple to show that this expression reduces to the cold beam result when $\Delta\to 0$. For small Δ,

$$\Lambda(\psi) = \frac{1}{\sqrt{1-\psi}} - 1 + \mathcal{O}(\Delta^2). \tag{15}$$

However, Eq. (14) is always nonsingular for $\Delta\neq 0$, which means that the singular point, $g=1$, that appears in the analysis of the preceding sections is now eliminated.

Equation (14) can be compared to Ref. 5, Eq. (5),

$$\rho(\psi) = 2\left[1+\frac{1}{\rho^2}\psi - \frac{1}{\sqrt{1-\psi}} - \frac{\Delta^2}{5}\,\frac{\psi}{(1-\psi)^{5/2}}\right], \tag{16}$$

where $\rho^{-2}\propto M^2$ is a constant to be determined, and the temperature normalization has been converted using $\alpha = 3.75/\Delta^2$, as that yields the best fit between the two model distributions. Equation (16) is derived from a Maxwellian distribution, rather than a Lorentzian as done here. However, Eq. (16) retains the singular behavior at $g=1$, which should have been eliminated once thermal effects were included. ψ in Eq. (16) is the same as g in the current problem, as the analysis has been reduced to a one-dimensional problem by assuming the perpendicular dependence to be $J_0(\lambda_{01} r/a)$. This is in contrast to Eq. (14) where ψ is still completely general. Given the Lorentzian distribution, the expression is exact.

The analysis of the preceding section can be repeated, with the warm plasma charge density given by Eq. (14). The resulting potential equation becomes

$$\frac{1}{2}\left(\frac{dg}{dz}\right)^2 - \frac{k_\perp^2 g^2}{2} = -\frac{\langle \psi_\perp | P \int_0^g \Lambda(u\psi_\perp)\,du\rangle}{\langle \psi_\perp | \psi_\perp\rangle}. \tag{17}$$

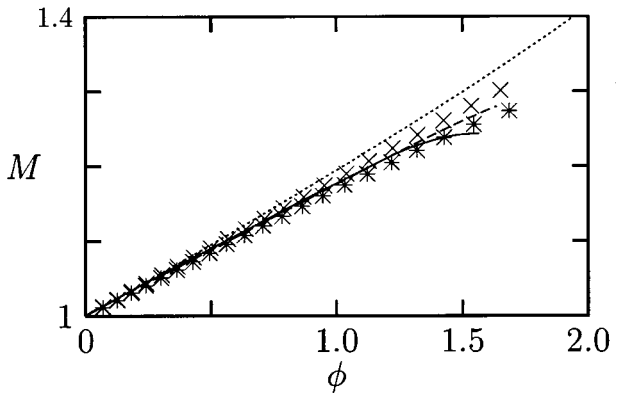

FIG. 4. Figure showing the Mach number, M, as a function of peak potential gM^2, for a warm plasma. The dotted line is the analytic cold result of Fig. 1. The dashed line is the equivalent result from Eq. (18) with $\Delta=0.15$. The $\times$ symbols correspond to the numerical procedure of Sec. III for the case of $\Delta=0$ and the asterisks correspond the the case of $\Delta=0.15$. These results are for the case where the plasma uniformly fills the chamber. The solid line is the result obtained in Ref. 6, Fig. 2, which is a result of numerically solving Eq. (1) on a grid. Note: The data from Ref. 6 was linearly scaled in ϕ to agree with the numerics in the linear limit.

Following the same arguments below Eq. (4), the following is obtained:

$$M^2=\frac{\beta(\Delta)}{g^2}\,\frac{\langle\psi_\perp|P\int_0^g\Lambda(u\psi_\perp)du\rangle}{\langle\psi_\perp|P\psi_\perp\rangle}, \tag{18}$$

where, for the case of a uniform plasma column ($P\equiv P_0$),

$$\frac{1}{\beta(\Delta)}=2\left[\frac{1}{1+(0.75\Delta)^2}-\frac{1}{2\sqrt{1+(0.75\Delta)^2}}\right] \tag{19}$$

is the quantity required to make $M\to 1$ as $\psi\to 0$. Equation (18) is analogous to Eq. (7) with V_g set to zero. The dashed line in Fig. 4 is obtained from Eq. (18) for a case of $\Delta=0.15$. As can be seen, the effect of temperature is to reduce the peak Mach number that can be achieved. It is worth noting that $\Lambda(\psi)$, which is defined in Eq. (14), needs to be evaluated with care as it involves some very delicate cancellations. The approach used was to fit the function using Chebyshev polynomial fits, which also solved the problem of evaluating the indefinite integral in Eq. (18) (Ref. 9, p. 190).

Equation (5) of Ref. 5 can also be used to generate a dispersion curve. When converted into a potential form, it yields [Ref. 5, Eq. (7)]

$$U(\psi)=C-2\left(\psi+\frac{\psi^2}{2\rho^2}+2\sqrt{1-\psi}+\frac{\Delta^2}{7.5}\,\frac{2-3\psi}{(1-\psi)^{3/2}}\right). \tag{20}$$

This equation, however, does not have the correct properties near $\psi=1^-$. Recognizing $\rho\propto M^{-2}$, Eq. (20) reduces to

$$M^2=C_1\Delta^2\frac{3\psi-2}{\psi^2(1-\psi)^{1.5}}+\cdots \tag{21}$$

near $\psi=1$ (C_1 is a positive constant). It is clear that M increases without bound near $\psi=1$, which is unacceptable.

IV. INCLUDING PERPENDICULAR NONLINEARITIES

In an earlier paper,[10] a technique was briefly presented to solve for the structure of the sheath due to an electron beam reflected by a potential barrier. This technique is elaborated here and applied to the problem of nonlinear waves.

The use of separation of variables in nonlinear problems is not new. The nonlinear Schrödinger equation has long been known to be exactly separable for certain types of nonlinearities.[11] The nonlinear equation in this paper,

$$\nabla_\perp^2\psi+\frac{\partial^2\psi}{\partial\zeta^2}=-P\Lambda(\psi), \tag{22}$$

where $\Lambda(\psi)$ is defined in Eq. (14), is not, however, exactly separable. However, an asymptotic treatment may be used on this problem that is analogous to that used in studies of planetary and solar magnetotails.[12] The idea that is exploited here is that the perpendicular structure is only a weak function of the parallel dependence, and to good accuracy may be parametrized by the mode amplitude at the current axial location:

$$\psi(\rho,\zeta)=g(\zeta)\psi_\perp(\rho,\epsilon g(\zeta)). \tag{23}$$

The scalelength on which g itself changes is quite short, since it decays exponentially away from the peak of the wave with a scalelength comparable to the perpendicular dimensions of the column. However, the perpendicular shape of the wave is seen in numerical studies[6,7] to vary but little and that too on the scalelength of the solitary wave width. When Eq. (23) is substituted into Eq. (22), we get

$$\frac{d^2g}{d\zeta^2}\psi_\perp+g\nabla_\perp^2\psi_\perp+g\frac{\partial}{\partial\zeta}\left(\frac{dg}{d\zeta}\frac{\partial\psi_\perp}{\partial g}\right)=-P\Lambda(g\psi_\perp). \tag{24}$$

The assumption of weak dependence of $\psi_\perp$ on g permits us to neglect the last term on the left-hand side of Eq. (24). This results in the following equation:

$$\frac{1}{g}\frac{d^2g}{d\zeta^2}=-\frac{\nabla_\perp^2\psi_\perp}{\psi_\perp}-\frac{P\Lambda(g\psi_\perp)}{g\psi_\perp}=\lambda. \tag{25}$$

The quantity λ is simultaneously equal to a quantity involving g and ζ and to a quantity involving $\psi_\perp$, g, and ρ. λ must therefore be a function of g alone. Two equations result from this,

$$\nabla_\perp^2\psi_\perp+\lambda(g)\psi_\perp=-\frac{P\Lambda(g\psi_\perp)}{g}, \tag{26}$$

$$\frac{d^2g}{d\zeta^2}-g\lambda(g)=0, \tag{27}$$

subject to the boundary conditions $\psi_\perp=0$ at $\rho=1$, $\psi_\perp=1$ at $\rho=0$, $\psi_\perp'=0$ at $\rho=0$, and $g\to 0$ as $\zeta\to\pm\infty$. Equation (26) is a nonlinear equation for the perpendicular eigenmode. Since the problem is overspecified, solutions exist only for specific λ. The solution of Eq. (26) can therefore be viewed as the problem of the determination of $\lambda(g)$. Once $\lambda(g)$ is available as a function, Eq. (27) reduces to a simple potential problem, with the effective potential now defined by

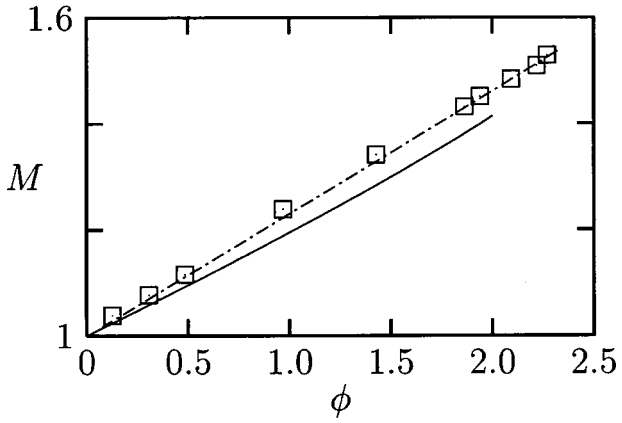

FIG. 5. Figure showing the Mach number, M, as a function of peak potential gM^2, for a cold, Cartesian plasma with a vacuum gap. The plasma is a uniform slab occupying the inner 44% of the volume. The squares are data obtained for this configuration from Ref. 7 (Fig. 5) via a PIC simulation. The solid line is the analytic result of Eq. (9), which is for a filled, cylindrical system. The dotted–dashed line is the result of the procedure described in Sec. IV for the same parameters as the PIC simulation. Note: The simulation data was linearly scaled along ϕ to agree with the numerics in the linear limit. Only the late time data is plotted, and $M=1$ has been defined as the small amplitude limiting value.

$$V_g(g) = -\int_0^g u\lambda(u)du. \tag{28}$$

The procedure described in Ref. 12 is only slightly different from this paper. In that treatment, the z dependence is available through algebraic relationships, and once the perpendicular equation is solved, the entire problem is done. Here, the solution of the perpendicular equation (26) leads into another equation, this time for $g(\zeta)$ itself.

Figure 4 displays the results of this procedure for two cases. The $\times$ symbols correspond to a case of $\Delta=0$, i.e., a cold plasma, and the asterisk symbols correspond to a case of $\Delta=0.15$. Since Δ^2 is proportional to the thermal energy spread in the distribution, it is expected that the singularity will soften as Δ increases. As seen from the figure, this is indeed the case.

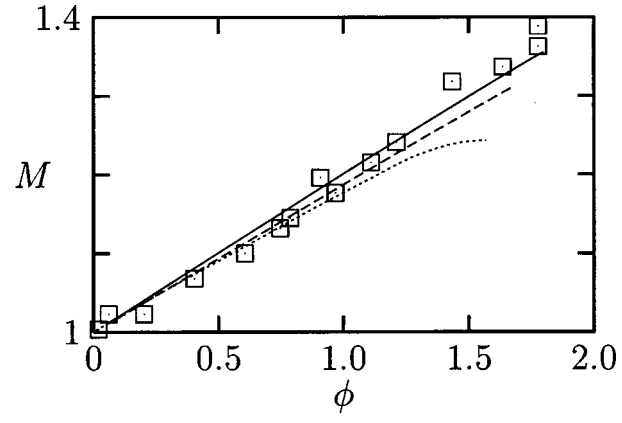

FIG. 6. Figure showing the Mach number, M, as a function of peak potential gM^2, for a cold, cylindrical plasma with different vacuum gaps. The squares are from Ref. 2, Fig. 7(a). The dashed line is for $r/a=0.75$ and the solid line is for $r/a=0.5$, where r is the plasma radius and a is the inner diameter of the wall. According to Ref. 2, the filament injector had a $r/a=0.75$. The dotted line is the result from Ref. 6, which corresponds to the case of $r/a=1$. Note: The imported data has been scaled in ϕ to agree in the linear limit.

The dotted line in Fig. 4 corresponds to the analytic result of Eq. (9). The agreement with the numerical result is quite poor. For the case of $\Delta=0.15$, the agreement between the the numerical procedure and the analytic result from Eq. (18) is quite good. The poor agreement for $\Delta=0$ is expected, since that is when the perpendicular profile is expected to distort the most. The solid line in the figure is the result from Ref. 6, Fig. 2. This is the result of numerically solving the elliptic equation (1) on a two-dimensional mesh using a finite-difference approximation of the Laplacian. There is a clear deviation at the higher values of M, where the procedure presented in this section yields a higher answer than that of Ref. 6.

Figure 5 presents the results for a plasma slab with a vacuum gap. To compare with the results of Ref. 7, Cartesian geometry was used in the numerical procedures. The PIC simulation results of Ref. 7 were for a case where the plasma occupied 44% of the volume of the chamber. The results are shown as squares in the figure. The dotted–dashed line corresponds to the same case solved by the procedure described in this section. The agreement is excellent. It should be noted that the crucial features are the shape of the curve and the highest value of M, Without the vacuum gap, the numerical procedure yields much lower values of M. The solid line is the analytic result of Eq. (9). This is now a case where the numerical solutions actually yield higher values than the analytical prediction.

Figure 6 presents the results of a cylindrical plasma with a vacuum gap. This is relavent to most experiments.[2,3] The squares are from Fig. 7(a) of Ref. 2. The solid line corresponds to a case of $r/a=0.5$, while the dashed line corresponds to $r/a=0.75$. According to Ref. 2, the injector size corresponded to the latter curve. However, it is quite likely that the plasma filled a smaller volume that that, which perhaps explains why the solid line fits the data better. The dotted line corresponding to Ref. 6 is well below the data, but that is partly because it corresponds to a filled waveguide, i.e., $r=a$.

The formulation developed in this paper was applied to the problem of a violently relaxing plasma that encounters a potential barrier.[10] The results of that study are briefly summarized here to highlight the strengths and weaknesses of method presented here.

Simulation of a quiescent non-neutral plasma column that is abruptly permitted to expand and equilibrate in a longer column indicates that as the plasma beams slow down, they develop internal sheaths, similar to double layers seen in neutral plasmas. The onset of these internal sheaths is quite predictable and they retain their ''shape'' for long periods of time. The formulation presented in this paper was applied to that problem, and the onset and evolution of the structures were successfully predicted.[10] The technique followed was exactly the same as that given in the preceding sections, except that in this problem, *all the electrons are*

trapped, and the potential structure is truly stationary in the laboratory frame.

A failing of the procedure, however, was in the detailed structure of the ''front'' itself. As expected, the WKB-like approach did not work well in describing the perpendicular profile in this region, with the actual profile being far smoother than the one generated by the procedure described here. However, this failing notwithstanding, the procedure predicted almost precisely the onset of this structure, and when fast electron contributions were accounted for, predicted the subsequent evolution perfectly.

V. CONCLUSIONS

In this paper we have presented a useful technique to extract the structure of two and three-dimensional electrostatic structures in plasma columns. The procedure permits the perpendicular response of the plasma to depend on the local amplitude of the wave, thereby improving on conventional treatments that assume that the perpendicular structure remains unchanged from its linear form. The method parallels a technique common in astrophysics, in the treatment of magnetotails.[12]

The conventional treatment that freezes the perpendicular profile of the wave has also been extended to obtain fully nonlinear solutions. It is found that they overestimate the wave-breaking Mach number for a filled waveguide, but predict reasonably the dispersion equation for solitons in a quarter-filled waveguide. Since most experiments work with $r/a \sim 0.5$, this is a fortunate coincidence that helps to explain the success of this simple theory.

The good agreement between the results obtained here and the experimental and numerical results in the literature suggest that the procedure is a robust one. It is easily generalized to systems with slowly changing cross sections and complex geometries.

While agreement has been obtained between the results of this procedure and prior work in the literature, one deviation does exist. The results of Ref. 6 does not agree for amplitudes near the wave breaking limit. This deviation requires further investigation.

A significant aspect of the work has been the use of a nonsingular charge density that exactly corresponds to a warm Lorentzian distribution for the electrons. This formulation permits this technique to be extended to the study of trapped populations as well, as has been presented by the authors in an earlier paper.[10]

ACKNOWLEDGMENT

The author wishes to acknowledge the many insights he received from Professor G. J. Morales, which lead to the formulation of this method for sheath studies.[10]

[1] H. Ikezi, P. J. Barrett, R. B. White, and A. Y. Wong, Phys. Fluids **14**, 1997 (1971).
[2] J. P. Lynov, P. Michelsen, H. L. Pecseli, J. J. Rasmussen, K. Saeki, and V. A. Turikov, Phys. Scr. **20**, 328 (1979).
[3] J. D. Moody and C. F. Driscoll, Phys. Plasmas **2**, 4482 (1995).
[4] A. W. Trivelpiece and R. W. Gould, J. Appl. Phys. **14**, 1784 (1959).
[5] I. M. Aleshin, L. S. Kuz'menkov, and O. O. Trubachev, Plasma Phys. Rep. **19**, 520 (1993).
[6] T. P. Hughes and E. Ott, Phys. Fluids **23**, 2265 (1980).
[7] S. C. Neu and G. J. Morales, Phys. Plasmas **2**, 3033 (1995).
[8] I. B. Bernstein, J. M. Greene, and M. D. Kruskal, Phys. Rev. **108**, 546 (1957).
[9] W. H. Press, S. A. Teukolsky, W. T. Vellerling, and B. P. Flannery, *Numerical Recipes in Fortran*, 2nd ed. (Cambridge University Press, New Delhi, 1993), pp. 184–190.
[10] H. Ramachandran, G. J. Morales, and V. K. Decyk, *Non-Neutral Plasma Physics II, Berkeley 1994*, AIP Conference Proceedings No. 331 (American Institute of Physics, Melville, NY, 1995), p. 155.
[11] V. E. Zakharov, V. V. Sobolev, and V. C. Synakh, Sov. Phys. JETP **33**, 77 (1971).
[12] T. Wiegelmann, K. Schindler, and T. Neukirch, Sol. Phys. **180**, 439 (1998), and references therein.